Journal of Ceramic Processing Research. Vol. 13, No. 2, pp. 188~192 (2012)

J O U R N A L O F
Ceramic Processing Research

Magnetic and electrical properties of BFO/PZT heterolayered thin films

Seung-Hwan Lee[a], Sung-Pill Nam[b], Seon-Gi Bae[c] and Young-Hie Lee[a,*]
[a]*Dept. of Electronics Materials Engineering, Kwangwoon University, Korea*
[b]*Dept. of Smart Grid Research, Korea Electrotechnology Research Institute, Korea*
[c]*Dept. of Electrical Engineering, University of Incheon, Korea*

$BiFeO_3$/PZT(20/80) (hereafter BFO/PZT) heterolayered thin films were deposited by an RF sputtering method on Pt/TiO_2/SiO_2/Si substrates. We investigated the effects of deposition conditions on the magnetic and electrical properties of BFO/PZT heterolayered thin films. The thickness of BFO/PZT heterolayered thin films is about 500 nm. All BFO/PZT films show a void free uniform grain structure without the presence of rosette structures. It can be assumed that the crystal growth of the upper BFO layers can be influenced by the lower PZT layers. This study suggests that the design of the BFO/PZT heterolayered thin films should be an effective method to enhance the magnetic and electrical performance in devices.

Key words: $BiFeO_3$/PZT(20/80), Thin films, RF sputtering method, Electrical properties.

Introduction

Multiferroic materials have recently attracted attention because of their potential use in devices. Because of the possible coupling between the magnetic and electronic structures the magnetization could be switched by applying an electric field, and the ferroelectric polarization switched by applying a magnetic field.

$BiFeO_3$ (BFO) materials exhibit a distorted perovskite structure with rhombohedral symmetry. They belongs to the R3c space group with a unit cell parameter a = 0.5634 nm and. a = 59.348° [2]. One of the striking features of BFO materials is the coexistence of ferroelectric (T_c = 1123 K) and antiferromagnetic orderings (T_N = 643 K) at room temperature due to a residual moment from a canted spin structure [3, 4]. In single crystals, the spontaneous polarization (P_s) is 3.5 C/cm^2 along the [001] direction, indicating a value of 6.1 C/cm^2 along the [111] direction at 77 K. Transport measurements in the bulk have been hampered by leakage problems, likely a result of defects and nonstoichiometry, which have limited the applications of this material. To overcome this obstacle, recent work has focused on solid solutions of $BiFeO_3$ with other ABO_3 materials, such as $BaTiO_3$, which can prevent second-phase formation and increase the sample resistivity [5]. It was considered that the ferroelectric fatigue is related to the pinning of oxygen vacancies or other point defects during ferroelectric domain switching [6]. As an efficient way, the concentration of oxygen vacancies accumulated in ferroelectric films can be reduced by using an oxide as an electrode. Some oxide/ferroelectric/oxide trilayer structures, for example, (Ba,Sr)TiO_3/Pb(Zr,Ti)O_3/(Ba,Sr)TiO_3 [7], (Bi,La)Ti_3O_{12}/Pb(Zr,Ti)O_3/(Bi,La)Ti_3O_{12} [8] and (Pb,La) TiO_3/Pb(Zr,Ti)O_3/(Pb,La)TiO_3 [9], exhibit better fatigue endurance characteristics. Recently, improved dielectric properties were found in a $BiFeO_3$/(Bi,La)Ti_3O_{12} bilayer [10]. And we have already reported on the good dielectric properties of PZT heterolayered films which they were alternately spin-coated using PZT(20/80) and PZT(80/20) metal alkoxide solutions [11].

In this study, BFO/PZT heterolayered thin films were deposited by an RF sputtering method on Pt/TiO_2/SiO_2/Si substrates. The magnetic and electrical properties of BFO/PZT heterolayered thin films were investigated with varying deposition temperatures ranging from 450 °C to 650 °C.

Experiments

The BFO/PZT heterolayered thin films were deposited on Pt/TiO_2/SiO_2/Si substrates by an RF sputtering method. The BFO and PZT targets were prepared by a conventional mixed oxide method. The starting materials were Bi_2O_3 (99.99%), Fe_2O_3 (99.99%), PbO (99.99%), ZrO_2 (99.99%) and TiO_2 (99.99%). These materials were weighed accoring to the composition of the $BiFeO_3$, $PbZrTiO_3$ (20/80) respectively. The weight ratio of zirconia balls to powder in the mill was 1 : 1 and ethyl alcohol was used as a process control agent. The slurry was dried at 120 °C for 24 h. The dried powders were screened by mesh (#325) and the screened powders were then pressed into disk samples of 12 mm diameter. The BFO and PZT targets were sintered at 900 °C, 1200 °C 2 h. respectively. The sintered ceramic target

*Corresponding author:
Tel : +82-2-915-80844
Fax: +82-2-915-80844
E-mail: yhlee@kw.ac.kr

Table 1. Sputtering conditions for the BFO/PZT heterolayered thin films

Target	$BiFeO_3/Pb(Zr_{0.2}Ti_{0.8})O_3$
Substrate	$Pt/TiO_2/SiO_2/Si$
RF power	100[W]
Deposition pressure	3.9×10^{-1} [Pa]
Deposition time	10 [minute]
Ar/O_2	50/20
Annealing temperatures	450, 500, 550, 600, 650 [°C]

was lapped and Pt paste was fired on the sample faces at 600 °C. The BFO/PZT heterolayered thin films were doomed by depositing the PZT and BFO targets alternately. And we investigated the magnetic and electrical properties with different deposition temperatures.

The vacuum chamber was evacuated down to pressure 3.9×10^{-4} Pa and the sputtering atmosphere was controlled by varying the deposition temperature at a total pressure of 3.9×10^{-1} Pa. The RF power for the targets was 100 W and the target-substrate distance was about 7 mm. The deposition conditions of the BFO/PZT heterolayered thin films are summarized in Table 1. The thickness of the films was measured using a field emission electron microscope (FESEM) and α step. The crystalline structures of the BFO/PZT heterolayered thin films were analyzed by X-ray diffraction (XRD). The surface and cross-sectional microstructures of the films were examined by a field emission scanning electron microscope (FESEM). For electrical measurements, an Au thin film was deposited by an evaporator at room temperature as the top electrode with a diameter of 0.1 mm. The dielectric constant and dielectric loss measurements were carried out using an LCR meter (PM6306, pluke) Hysteresis loops of the samples were measured by a RT66A ferroelectric test system. The magnetization was measured using a superconducting quantum interference device (SQUID) (MPMS XL-7).

Results and Discussion

The XRD patterns of the BFO/PZT heterolayered thin films deposited on $Pt/TiO_2/SiO_2/Si$ substrates with different deposition temperatures ranging from 450 °C to 650 °C are shown in Fig. 1. In all samples, the diffraction peaks correspond to the perovskite structures of BFO and PZT (the peaks of rhombohedral and tetragonal). The presence of some pyrochlore phase can be observed such as Fe_2O_3, $Bi_{25}FeO_{39}$, $Bi_{36}Fe_{24}O_{57}$ and $Bi_2Fe_4O_9$. As reported, BFO/PZT thin films have a high (110) preferred orientation, while it could not be distinguished because of overlapping with the Pt (111) peak. However, the characteristic peaks (012), (110), (116), (200) peaks can be observed. As shown in the Fig. 1, as the deposition temperature increases to 550 °C, the BFO/PZT heterolayered thin film begins to crystallize. The intensities of the BFO/PZT heterolayered

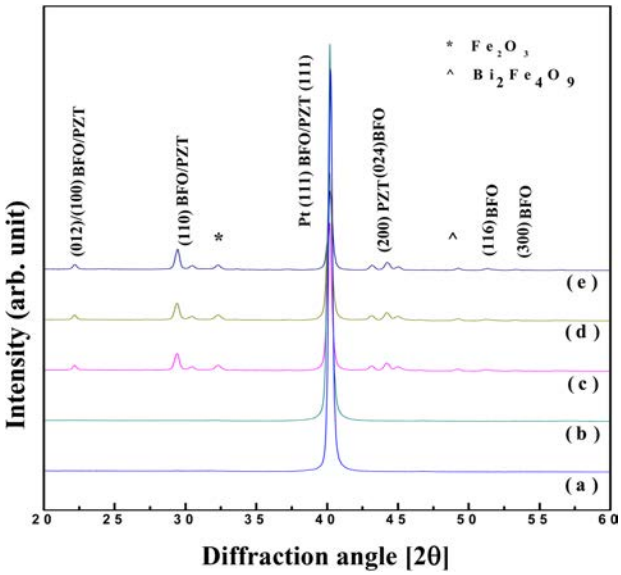

Fig. 1. XRD patterns of BFO/PZT heterolayered thin films deposited with different deposition temperatures. (a) 450 °C, (b) 500 °C, (c) 550 °C, (d) 600 °C, (e) 650 °C.

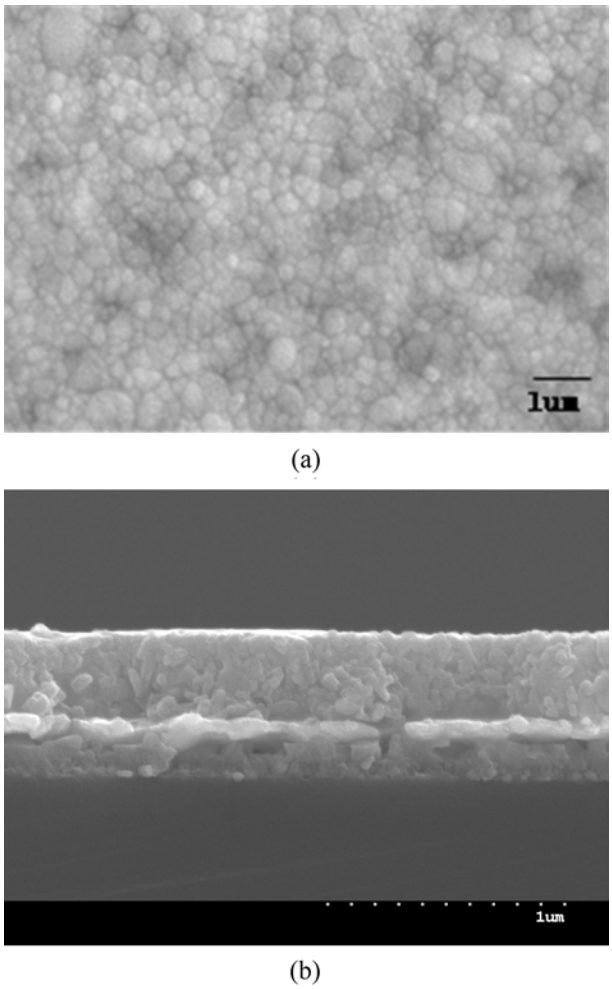

Fig. 2. FE-SEM images of the surface and cross-sectional-structurals for the BFO/PZT heterolayered thin films deposited at 600 °C.

thin films deposited at 650 °C were larger compared with those of the other BFO/PZT heterolayered thin films.

The microstructure of the BFO/PZT heterolayerd thin films deposited on $Pt/TiO_2/SiO_2/Si$ substrates was further investigated by FESEM. Fig. 2 shows the crack-free surface morphology of BFO/PZT heterolayerd thin films annealed at 600 °C and the cross-section analysis reveals that the BFO/PZT heterolayrered thin film deposited under the same conditions are dense. The separation interface between BFO and PZT layers are not clear owing to the insignificant difference in the contrast of the component materials. The thickness of films was approximately 500 nm and this thin film was dense, indicating a good structure had been obtained. The grain size of the BFO/PZT heterolayered thin film deposited at 600 °C was from 0.1 to 0.2 μm. BFO/PZT heterolayered thin films showed a uniform grain structure and void free grain structure without the presence of a rosette microstructure. The improvement in the structure of BFO/PZT heterolayered thin films was considered to be an important factor as to why the ferroelectric and magnetic properties are improved by the inducing ferroelectric layer. The Pt/SiO_2 interfaces became very rough interfacial layers. This phenomenon can be probably explained by the fact that the diffusion of Pb from the PZT film into the Pt bottom electrode and the diffusion of Ti are severely advanced through the several annealing processes. And Pb diffusion becomes exacerbated in PZT films containing higher concentrations of Zr.

Fig. 3 shows the frequency dependences of the relative dielectric constant and dielectric loss of the BFO/PZT heterolayered thin films from 1 kHz to 1 MHz. Because the dielectric constant of BFO is much smaller than PZT, the average dielectric constants of BFO/PZT heterolatered thin films are smaller than for PZT thin films. When the frequency increases, the dielectric constant significantly decreases below 10 kHz. There is no change in the dielectric constant above 10 kHz. However, dielectric constant decrease again above 700 kHz. The dielectric constant and dielectric loss are increased with an

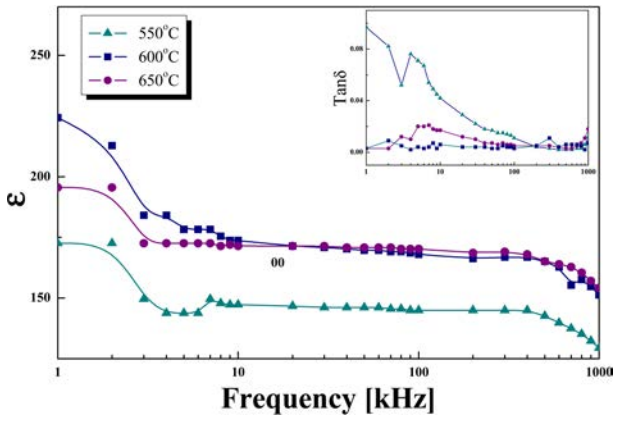

Fig. 3. Frequency dependence of the dielectric properties of BFO/PZT heterolayered thin films.

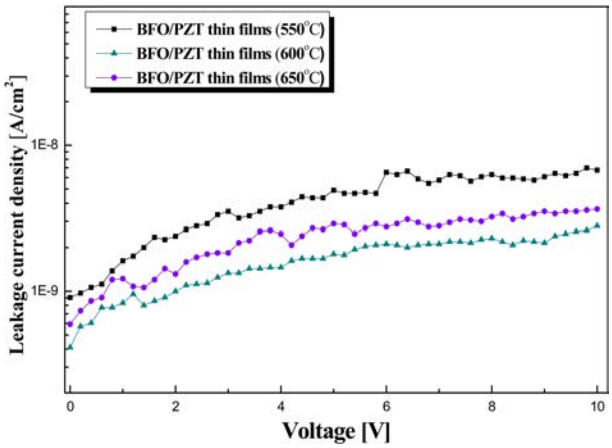

Fig. 4. Leakage current densities of BFO/PZT heterolayered thin films.

increase in the deposition temperature. It is well known that the dielectric loss is affected by various factors such as a secondary phase, and the pyrochlore phase. BFO/PZT heterolayered thin films exhibit a superior dielectric constant compared with the single composition BFO (200 at 1 KHz) and PZT (95/5) (358 at 100 KHz) thin films. We consider that the rhombohedral structure of BFO films ($a = 0.5634$ nm) was distorted due to the large lattice mismatch and compressive stress imposed by the lower orthorhombic PZT film ($a = 0.4149$ nm, $c = 0.4112$ nm). Therefore, BFO/PZT heterolayered thin films showed good dielectric properties because of the large ionic displacements in the distorted perovskite structure. This dielectric dispersion results from the interfacial polarization, namely the Maxwell-Wagner relation caused by space charge polarization in film/electrode and film/film interfaces.

Fig. 4 shows the leakage current densities of the PZT heterolayered thin films with applied voltage. As expected, leakage current densities decrease with an increase in the deposition temperature and leakage current densities of BFO/PZT heterolayered thin films were lower in value than those of single composition BFO thin films. These results suggest that trap centers of carriers were formed at the interface between the BFO film and PZT (20/80) film and were decreased with an increase in the deposition temperature. The leakage current density of the BFO/PZT heterolayered thin films annealed at 600 °C is less than 1.74×10^{-9} A/cm^2 at 5 V. These values are small enough for their application in memory devices.

Fig. 5 shows the P-E hysteresis loops of the BFO/PZT heterolayered thin films. It is evident that the remanent polarization and saturation polarization of the BFO/PZT heterolayered thin films are proportional to the deposition temperature and remanent polarizations of BFO/PZT heterolayered thin films deposited at 500 °C, 550 °C and 600 °C are 2.6 μC/cm^2, 4.9 μC/cm^2 and 10.1 μC/cm^2 respectively, which is bigger than the value of pure BFO. Compared with the loop of ferroelectric

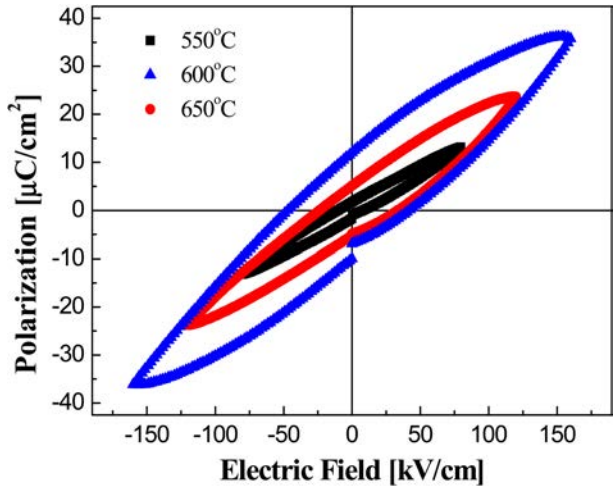

Fig. 5. Ferroelectric hysteresis loops of BFO/PZT heterolayered thin films.

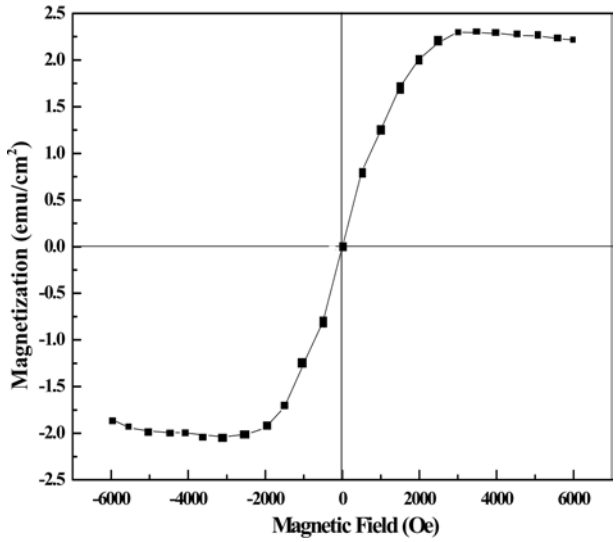

Fig. 6. Variation of magnetization with magnetic field for BFO/PZT heterolayered thin films deposited at 600 ℃.

thin films, the shape of P-E hysteresis loops of BFO/PZT heterolayered thin films is like a parallelogram. It is well known that an ideal P-E loop of ferroelectrics is like a rectangle. The difference between the P-E hysteresis loops of BFO/PZT heterolayered thin films and PZT thin films shows that the defects produce more effects in the BFO/PZT heterolayered thin films than in the PZT thin films.

Magnetization-magnetic field characteristics of BFO/PZT heterolayered deposited at 600 °C were carried out at room temperatures. The magnetic hysteresis loop is shown in Fig. 6, which shows that BFO/PZT heterolayered thin films exhibit magnetic order in the materials at room temperature. It is obvious that BFO/PZT heterolayered thin films are antiferromagnetic. The saturation magnetization is about 2.3 emu/cm^3. This indicates that magnetization is not improved by the strain between BFO and PZT layers.

Conclusions

In this paper, BFO/PZT hereolayered thin films, which were deposited on the Pt/Ti/SiO_2/Si substrates, were prepared by an RF sputtering method. The magnetic and electrical properties of the BFO/PZT heterolayered thin films were studied. All films showed a uniform grain structure without the presence of a rosette structure. It can be assumed that the crystal growth of the upper BFO layers can be influenced by the lower PZT layers. Dielectric and ferroelectric properties of BFO/PZT heterolayered thin films were much better than those of a single composition BFO film and the remanent polarization and saturation magnetization of the BFO/PZT heterolayered thin films deposited at 600 °C are 10.1 μC/cm^2, and 2.3 emu/cm^3. We consider that these properties of BFO/PZT heterolayered thin films are caused by the distorted rhombohedral crystal structure of the BFO film due to the compressive stress imposed by the lower PZT film. BFO/PZT heterolayered films showed typical dielectric dispersion properties, which indicates that interfacial polarization was caused by space charges in the film/film and film/electrode interfaces. However, further investigations and discussions are necessary to understand the interfacial characteristics and ferroelectric response in the BFO/PZT heterolayered thin films.

References

1. B. Jaffe, W.R. Cook, and H. Jaffe, Piezoelectric Ceramics, Academic Press (New York, 1971).
2. F. Kubel and H. Schmid, Acta. Crystallogr. B 46 (1990) 698.
3. F. Bai, J. Wang, M. Wuttig, J. Li, N. Wang, A.P. Pyatakov, K.K. Zvezdin, L.E. Cross, and D. Viehland, Appl. Phys. Lett. 86 (2005) 032511.
4. F. Zavaliche, P. Shafer, R. Ramesh, M.P. Cruz, R.R. Das, D.M. Kim, and C.B. Ean, Appl. Phys. Lett. 87 (2005) 252902.
5. K. Ueda, H. Tabata, and T. Kawai, App. Phys. Lett. 75 (1999) 555.
6. O. Auciello, J.F. Scott, and R. Ramesh, Phys. Today 51 (1998) 22.
7. F. Yan, Y.N. Wang, H.L.W. China, and C.L. Choy, Appl. Phys. Lett. 82 (2003) 4325.
8. D.H. Bao, X.H. Zhu, S.K. Lee, M. Alexe, and D. Hesse, Appl. Phys. Lett. 86 (2005) 082906.
9. E.S. Lee, H.W. Chung, S.H. Lim, and S.Y. Lee, Appl. Phys. Lett. 86 (2005) 032093.
10. F.Z. Hung, X.M. Lu, W.W. Lin, W. Cai, X.M. Wu, Y. Kan, H. Sang, and J.S. Zhu, Appl. Phys. Lett. 90 (2007) 252903.
11. S.G. Lee and Y.H. Lee, Trans. Electr. Electron. Mater. 6(2) (2005) 35-38.
12. W. Wang, T. Karaki, and M. Adachi, Jpn. J. Appl. Phys. 37 (1998) 4910.
13. L.N. Chapin and S.A. Myers, Mater. Res. Soc. Symp. Proc. 200 (2000) 153.
14. S.G. Lee and Y.H. Lee, Thin Solid Films 353 (1999) 244.

15. G. Shirane, K. Suzuki, and A. Takeda, J. Phys. Soc. Jpn. 7 (1952) 12.
16. T.P. Gujar, V.R. Shinde, S.S. Kulkarni, H.M. Pathan, and C.D. Lokhande, Applied Surface Science 252 (2006) 3585.
17. J. Wang, J.B. Neaton, H. Zheng, V. Nagarajan, S.B. Ogale, B. Liu, D. Viehlan, V. Vaithyanathan, D.G. Schlom, U.V. Waghmare, N.A. Spaldin, K.M. Rabe, M. Wuttig, and R. Ramesh, Science 299 (2003) 1719.
18. P. Lunkenheimer, V Bobnar, A.V. Pronin, A.I. Ritus, A.A. Volkov, and A. Loidl, Phys Rev. B 66 (2002) 052105.